

CNRS - Université Pierre et Marie Curie - Université Versailles-Saint-Quentin
CEA - ORSTOM - Ecole Normale Supérieure - Ecole Polytechnique

Institut Pierre Simon Laplace

des Sciences de l'Environnement Global

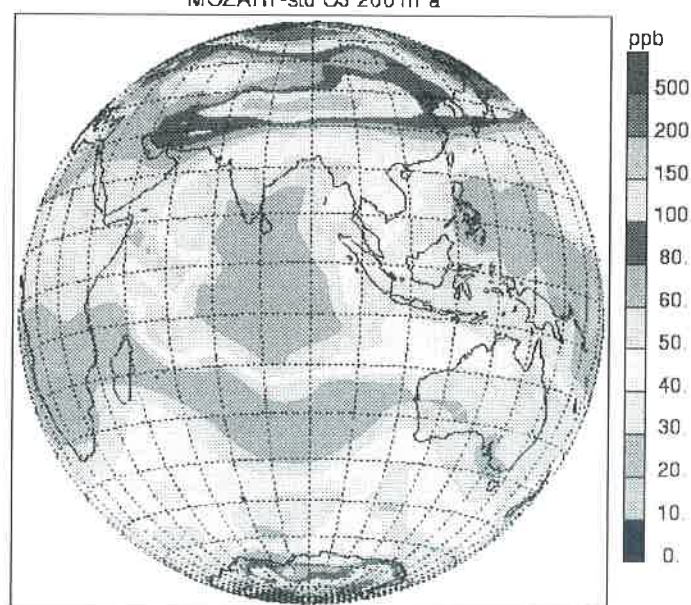
Notes du Pôle de Modélisation

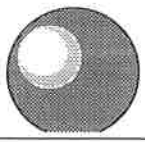
Impact of Biomass Burning and Lightning Emissions on the Distribution of Tropospheric Ozone and its Precursors in the Tropics

D. Hauglustaine

Service d'Aéronomie du CNRS

MOZART-std O3 200 hPa



 I P S L	CNRS - Université Pierre et Marie Curie - Université Versailles-Saint-Quentin CEA - CNES - ORSTOM - Ecole Normale Supérieure - Ecole Polytechnique
	Institut Pierre Simon Laplace des Sciences de l'Environnement Global
	CETP - LMD - LODYC - LPCM - LSCE - SA

Université Pierre-et-Marie-Curie B 102 - T15-E5 - 4, Place Jussieu 75252 Paris Cedex 05 (France) Tél : (33) 01 44 27 39 83 Fax : (33) 01 44 27 37 76	Université Versailles-Saint-Quentin Collège Vauban, 47 Boulevard Vauban 78047 Guyancourt Cedex (France) Tél : (33) 01 39 25 58 17 Fax : (33) 01 39 25 58 22
---	--

Impact of Biomass Burning and Lightning Emissions on the Distribution of Tropospheric Ozone and its Precursors in the Tropics

D. Hauglustaine

Service d'Aéronomie du CNRS

La combustion de la biomasse tropicale est une source importante de composés chimiques conduisant à la production photochimique de l'ozone dans la troposphère. Dans ce travail, deux aspects particuliers de l'impact de la combustion de la biomasse tropicale sont étudiés à l'aide d'un modèle tri-dimensionnel de chimie-transport calculant la distribution des espèces chimiques dans la troposphère (MOZART, Model for OZone And Related chemical Tracers).

Dans une première partie, le modèle MOZART a été utilisé pour simuler l'effet sur la composition de la troposphère des feux survenus au Kalimantan et Sumatra, Indonésie en 1997. Comme conséquence de l'émission importante de monoxyde de carbone par les feux de forêts et de tourbières, CO augmente de plus de 800 ppbv dans la troposphère libre au-dessus de l'Indonésie. Suite à la production photochimique accrue, l'ozone augmente de 20-25 unités Dobson dans la troposphère et atteint 60-70 ppbv dans la troposphère libre. Le transport vertical des polluants en dehors de la couche limite par convection et leur redistribution par les processus de transport de grande échelle induisent une perturbation de la composition chimique à l'échelle régionale dans tout le bassin Indonésien.

Mars 1999
Note n° 14

Dans une seconde partie, des sondages d'ozone effectués dans l'océan Indien durant quatre années consécutives entre 1987 et 1990 sont présentés. Ces mesures font apparaître des valeurs élevées d'ozone entre 5 et 10 km dans la bande de latitude 20-40S. Ce maximum contraste avec les rapports de mélange inférieurs à 20 ppbv observés dans les régions équatoriales. L'analyse des résultats du modèle MOZART montre que ce maximum d'ozone est associé à un vaste panache émanant des régions de feux de biomasse en Afrique. Nos résultats mettent en évidence l'importance des émissions d'oxydes d'azote par les éclairs sur la production photochimique de l'ozone dans la haute troposphère et la formation de panaches tels que ceux qui sont observés au dessus de l'océan Indien.

Partie 1

Changes in tropospheric ozone and its precursors during the 1997 fires in Kalimantan and Sumatra, Indonesia

D. A. Hauglustaine

Service d'Aéronomie du CNRS, Université de Paris 6, Paris, France

G. P. Brasseur

National Center for Atmospheric Research, Boulder, CO, USA

and

J. S. Levine

Atmospheric Sciences Division, NASA Langley Research Center, Hampton, VA, USA

Abstract. A global chemical transport model, called MOZART, is used to investigate the impact of the 1997 Indonesian fires on the distribution of tropospheric ozone and its precursors in the tropics. Due to the high release of carbon monoxide by the peat fires, CO increases by up to 800 ppbv in the free troposphere over Indonesia. As a consequence of increased photochemical production, ozone is significantly perturbed over the source region (Sumatra and Kalimantan). The tropospheric O₃ column increases by 20-25 DU and the mixing ratio of ozone reaches 60-70 ppbv in the mid-troposphere in November. Due to venting of pollutants out of the boundary layer and their subsequent redistribution by large-scale transport processes, the simulations indicate a significant impact of this local event on the composition of free troposphere on the regional scale.

1. Introduction

Deforestation in the tropics plays an important role in releasing large amounts of CO₂ into the atmosphere [Seiler and Crutzen, 1980; Crutzen et al., 1989]. Biomass burning is also a significant source of chemically active trace gases (e.g., CO, CH₄, non methane hydrocarbons, NO_x) leading to the photochemical production of tropospheric ozone [Crutzen et al., 1979]. Indirect satellite, aircraft, and ground based measurements have identified plumes of ozone emanating from South America and Africa during the biomass burning season [Fishman et al., 1991 ; Andreae et al., 1992; Thompson et al., 1996; Kim and Newchurch, 1996 ; Blake et al., 1999]. In 1997, unprecedented widespread fires occurred in Indonesia, starting in June-July and lasting for several months. Most of the fires were set by land owners, commercial loggers

and small farmers in attempts to clear and cultivate the land as already done in the past. However, the severe drought induced by a strong El Niño event could not help extinguish the fires and wash out the smoke and haze. Due to the release of significant amount of trace gases and particles, these fires profoundly affected the chemical composition of the troposphere on a regional scale.

In this paper, we use a global three-dimensional chemical transport model, called MOZART, to investigate the sensitivity of the calculated distribution of tropospheric ozone and its precursors to estimated biomass burning emissions associated with the 1997 Indonesian fires. The performed calculations are mainly aimed at testing the ability of a state-of-the-art global chemical transport model to reproduce the impact of biomass burning emissions on the composition of the troposphere in a specific case. A brief description of the model and considered emission scenario is given in section 2. The results are discussed in section 3, and concluding remarks are given in section 4.

2. Model Simulations

MOZART (Model for OZone And Related chemical Tracers) is a three-dimensional chemical transport model of the global troposphere described and evaluated by Brasseur et al. [1998] and Hauglustaine et al. [1998]. In MOZART (version 1), the time history of 56 chemical species is calculated on the global scale from the surface to the mid-stratosphere. The chemical scheme includes 140 chemical and photochemical reactions and considers the photochemical oxidation schemes of methane (CH_4), ethane (C_2H_6), propane (C_3H_8), ethylene (C_2H_4), propylene (C_3H_6), isoprene (C_5H_8), terpenes (as α -pinene, $\text{C}_{10}\text{H}_{16}$), and a lumped compound *n*-butane (C_4H_{10}) used as a surrogate for heavier hydrocarbons. The model is run on a horizontal T42 resolution corresponding to about 2.8 degrees in both latitude and longitude (about $300 \times 300 \text{ km}^2$ in the tropics). In the vertical, the model uses 25 levels extending from the surface to the level of 3 mb. Dynamical and other physical variables needed to calculate the resolved advective transport as well as smaller-scale exchanges and wet scavenging are pre-calculated by the NCAR Community Climate Model (version 2, $\Omega 0.5$ library), and provided every 3 hours from pre-established history tapes.

The biomass burning emissions associated with the 1997 Indonesian fires are introduced in MOZART on the basis of the emissions estimated by Levine et al. [1999]. Liew et al. [1998] estimated a total burned area of $45,600 \text{ km}^2$ (4.5 million hectares) for the Sumatra and

Kalimantan regions and for the period of August 1997 to December 1997. The burned area consists of 50% of agricultural and plantation areas, 30% of forests and bushes, and 20% of peat swamp forests [Levine et al., 1999]. The CO₂ release totals 191.48 TgC for the whole period and different ecosystems. Emission of other species are calculated on the basis of the CO₂ released and the emission ratios relative to CO₂ [Yokelson et al., 1997; Levine et al., 1999]. The estimated total emissions for the 1997 Indonesian fires are given in Table 1 and compared to the global and annual biomass burning emissions in the model. For CO and non methane hydrocarbons (NMHCs), the Indonesian fires contribute for about 10% of the annual and global biomass burning emission. High NO_x release is estimated for the peat fires, leading to an emission during the 1997 fires corresponding to about 80% of the global and annual mean considered in the base case simulation. In the model, the Indonesian emissions are introduced in 4 grid-cells, 2 grid-cells located in Sumatra and 2 in Kalimantan. The experiment is conducted during 5 months (August 1st to December 31st), assuming constant emissions from the fires during the entire simulation.

Particulate levels over the Indonesian region were particularly high during the 1997 fires, leading to the formation of persistent smoke plumes and haze. The smoke plumes, mainly located in the boundary layer, cause a direct radiative forcing scattering the solar radiation back to the free troposphere. Consequently, smoke particles have an impact on the photolysis rates and potentially on tropospheric ozone photochemical production and destruction rates. A discrete ordinates radiative transfer model [Madronich et al., 1999] has been used to illustrate the effect of smoke aerosols on photolysis rates. We consider a uniform aerosol layer in the boundary layer (0 to 2 km). Single-scattering albedo (ω_0) for smoke particles has been measured by Hobbs et al. [1997] in regional hazes at three locations in Brazil. They report a range for ω_0 of 0.82 to 0.84 at 550 nm and 0.88 when a humidity factor is applied. In this study, we assume a wavelength independent value $\omega_0=0.88$. Figure 1 shows the change in NO₂ photolysis rate for an aerosol optical depth $\tau=1, 2, 3$ and 4, averaged over the boundary layer height and in the free troposphere. In the boundary layer, due to increased absorption of solar radiation by aerosols, j_{NO_2} (and j_{O_3} , not shown) are decreased relative to aerosol-free conditions. For an optical depth of 3 (assumed conditions prevailing during the Indonesian fires), a decrease of the photolysis rates of about 35% is calculated for overhead sun conditions. In contrast, due to increased back scattering, j_{NO_2} (and j_{O_3}) are increased in the free troposphere by about 6 % for high-sun conditions ($\tau=3$). A correction factor of 0.7 in the

boundary layer (surface up to 2 km) and of 1.06 in the free troposphere (2 km to 12 km) is applied in MOZART to the aerosol free photolysis rates to account for the effect of smoke aerosols over the Indonesian region (7°S-7°N in latitude and 100°E-115°E in longitude).

3. Results

The change in tropospheric ozone column (O_3 integrated from the surface up to the model tropopause) when Indonesian emissions are considered is shown in Figure 2a on November 25. The change in ozone reaches a maximum of 24 DU (Dobson Unit) over Sumatra and Kalimantan. The magnitude of the ozone change is in line with the Earth Probe/TOMS measurements over the source region, which indicate tropospheric columns increasing from about 30-40 DU in 1996 to about 50-60 DU in 1997 over the Indonesian region (increase of about 20-30 DU) [Hudson and Thompson, 1998; Chandra et al., 1998]. Transport of ozone and precursors in this version of the model driven by the NCAR CCM dynamics shows an eastward flow to the Pacific ocean, and ozone increases by about 2-4 DU over the western Pacific. As illustrated by Hauglustaine et al. (1999) the change in the photolysis rates considered in the simulation (Fig. 1) reduces the photochemical activity in the boundary layer. Consequently, the maximum change in total ozone is decreased by about 2 DU in comparison to a sensitivity simulation neglecting the impact of aerosols on photolysis rates (not shown). Due to the high release of NO_x by the peat fires (Table 1), the NO_2 column increases by 20×10^{16} molec./cm² over Sumatra and Kalimantan (Fig. 2b). Due to the short NO_2 lifetime in the tropical boundary layer (typically less than a day over biomass burning regions [Jacob et al., 1996]), the change in NO_2 rapidly decreases away from the source region. At the surface, an increase in ozone mixing ratio reaching 33 ppbv is calculated in November over the Indonesian region (Fig. 2c). Due to the short lifetime of ozone in the tropics at the surface (about a week), the maximum increase is mainly localized over Sumatra and Kalimantan. Over the ocean, the ozone enhancement decreases rapidly due to ozone photochemical destruction in the marine boundary layer. In the free troposphere (500 mb), the ozone increase reaches a maximum of about 45 ppbv over Indonesia (Fig. 2d). Due to the longer lifetime of ozone at this altitude (about a month), an export occurs towards the North-East and plumes with enhanced ozone (increase of 10-20 ppbv) reach the Indo-China peninsula. Export of ozone south of the source region is also visible. Carbon monoxide increases by up to 2900 ppbv at the surface over Sumatra and Kalimantan (Fig. 2e). A perturbation of 50-100 ppbv is

calculated over the whole Indonesian region. In the free troposphere (Fig. 2f), CO increases by 800 ppbv over Indonesia due to the upward transport prevailing in this region and by about 80-100 ppbv over Thailand. In the free troposphere, the zonal winds are more intense and the transport as simulated by the CCM is characterized by a strong export to Indo-China and the Pacific ocean. The calculated CO increase reaches about 20-40 ppbv over the western Pacific. It should be kept in mind that the dynamics calculated by the NCAR CCM and used to drive the transport in MOZART represents mean conditions that are not necessarily representative of the actual conditions prevailing in 1997. However, the results clearly emphasize the impact of the fires on the composition of the free troposphere on a regional scale.

Figure 3 compares typical profiles of O_3 , CO, NO_x and peroxyacetyl nitrate (PAN) calculated for the base case simulation together with the profiles simulated during the 1997 fires. The profiles are geographically averaged over the region 1.5°S-1.5°N in latitude and 107°E-110°E in longitude. During the 1997 fires ozone reaches a maximum of 70 ppbv at the top of the boundary layer and 60 ppbv in the free troposphere in comparison to 30-40 ppbv in the base case simulation. Due to vertical mixing, carbon monoxide is fairly constant with altitude in the base case simulation with a value of about 100 ppbv throughout the troposphere. In the 1997 fires simulation, due to high CO release by the peat fires and photochemical production through NMHC oxidation, a mixing ratio of 350 ppbv is calculated at the top of the boundary layer. In the boundary layer where CO oxidation by OH prevails, the carbon monoxide mixing ratio reaches 250 ppbv. High mixing ratios (250 ppbv) are also calculated in the upper troposphere due to vigorous transport from the boundary layer to higher altitudes by convection.

The nitrogen budget is also considerably affected over Indonesia during the fires. In the base case (no emissions from the 1997 fires), the NO_x profile shows a « C-shape » with values of about 200 pptv at the surface, decreasing to 50 pptv in the mid-troposphere and increasing with height above 9 km. In the fire experiment, higher values of 1000 pptv are calculated in the boundary layer due to direct emission by the fires. The mixing ratio rapidly decreases with height due to conversion of NO_x to less reactive species (PAN, HNO_3). In the upper troposphere a secondary maximum of 800 pptv is also calculated due to vertical mixing through convective processes. PAN is formed by the reaction of peroxyacetyl radicals (issued from the NMHC oxidation chain) with NO_2 . A significant increase in PAN is calculated and associated with both increased NO_2 and NMHC concentrations. The mixing ratio ranges from about 200 pptv at the surface to 600 pptv at 3-4 km in the perturbation case. A secondary

maximum is also calculated in the upper troposphere (reaching 450 pptv) where PAN is more stable regarding thermal decomposition.

4. Conclusions

In this study, a global three-dimensional chemical transport model (CTM) is used to assess the impact of widespread fires in the tropics on the composition of the troposphere. A sensitivity simulation is conducted to illustrate the change in tropospheric ozone and its precursors associated with the 1997 Indonesian fires. This study is mainly aimed at testing the ability of a state-of-the-art CTM to simulate the change in tropospheric ozone in a specific biomass burning case. Due to the high release of carbon monoxide by the peat fires, CO increases by to 800 ppbv in the free troposphere over Indonesia. As a consequence of enhanced photochemical production, the tropospheric ozone column increases by 20-25 DU over the source region and the ozone mixing ratio reaches 70 ppbv in the mid-troposphere over Indonesia. The MOZART off-line chemical transport model used for the simulations is driven by dynamical fields calculated by the NCAR Community Climate Model. Therefore, the simulations are characterized by a mean climatological state instead of the actual meteorological conditions prevailing during the 1997 fire period. As a consequence, the transport of species in the model is mainly dominated by a strong export from the source region to the Pacific ocean in the free troposphere when export to India was actually observed in 1997. Note also, that the change in tropical convection associated with the 1997-1998 El Niño and illustrated by Chandra et al. [1998] is not included in our simulation. A version of MOZART driven by assimilated dynamical and physical fields is currently under development and should help to address this issue.

Despite this limitation, the results clearly show that the budget of carbon monoxide, NMHCs, nitrogen species, and ozone are profoundly affected by the fires in the boundary layer, but also in the free troposphere due to upward transport and subsequent redistribution of pollutants by large scale transport processes in the tropics. The simulation indicates a strong impact of this local event on the composition of the free troposphere on a the regional scale, stressing the need for accurate biomass burning emissions (i.e., fire location and extent, burned area, type of ecosystem burned and emission factors, timing of the fires) in chemical transport models.

Acknowledgments. Helpful discussions with S. Madronich and S. Walters are gratefully acknowledged. The National Center for Atmospheric Research is operated by the University Corporation for Atmospheric Research under the sponsorship of the National Science Foundation.

References

Andreae, M. O., A. Chapuis, B. Gros, J. Fontan, G. Helas, C. Justice, Y. J. Kaufman, A. Minga, and D. Nganga, Ozone and Aitken nuclei over equatorial Africa: airborne observations during DECAFE 88, *J. Geophys. Res.*, 97, 6137-6148, 1992.

Blake, D. R., et al., The pervasive influence of biomass burning on the mid-troposphere over the remote South central Pacific, *Science*, in press, 1999.

Brasseur G. P., D. A. Hauglustaine, S. Walters, P. J. Rasch, J.-F. Müller, C. Granier, and X.-X. Tie, MOZART: a global chemical transport model for ozone and related chemical tracers, Part 1. Model description, *J. Geophys. Res.*, 103, 28,265-28,289, 1998.

Chandra, S., J. R. Ziemke, W. Min, and W. G. Read, Effects of 1997-1998 El Niño on tropospheric ozone and water vapor, *Geophys. Res. Lett.*, 25, 3867-3870, 1998.

Crutzen, P. J., L. E. Heidt, J. P. Krasnec, W. H. Pollock, and W. Seiler, Biomass burning as a source of atmospheric gases CO, H₂, N₂O, NO, CH₃Cl, and COS, *Nature*, 282, 253-256, 1979.

Crutzen, P. J., W. M. Hao, M. H. Liu, J. M. Lobert, and D. Scharffe, Emissions of CO₂ and other trace gases to the atmosphere from fires in the tropics, in *Our changing atmosphere*, P. J. Crutzen, J.-C. Gérard and R. Zander (eds), pp. 449-471, Univ. of Liège, Liège, Belgium, 1989.

Fishman, J., K. Fakhruzzaman, B. Gross, D. Nganga, Identification of widespread pollution in the southern hemisphere deduced from satellite analysis, *Science*, 252, 1693-1696, 1991.

Hauglustaine D. A., G. P. Brasseur, S. Walters, P. J. Rasch, J.-F. Müller, L. K. Emmons and M. A. Carroll, MOZART: a global chemical transport model for ozone and related chemical tracers, Part 2. Model description, *J. Geophys. Res.*, 103, 28,291-28,335, 1998.

Hauglustaine D. A., G. P. Brasseur, and J. S. Levine, Impact of the 1997 Indonesian fires on tropospheric ozone and its precursors, Proceedings of the Wengen-98 Workshop on Biomass burning and its interactions with the Climate system, *in press*, 1999.

Hobbs, P. V., J. S. Reid, R. A. Kotchenruther, R. J. Ferrek, and R. Weiss, Direct radiative forcing by smoke from biomass burning, *Science*, 275, 1776-1778, 1997.

Hudson, R. D., and A. M. Thompson, Tropical tropospheric ozone from total ozone mapping spectrometer by a modified residual method, *J. Geophys. Res.*, 103, 22,129-22,146, 1998.

Jacob, D. J., et al., Origin of ozone and NO_x in the tropical troposphere : a photochemical analysis of aircraft observations over the South Atlantic basin, *J. Geophys. Res.*, 101, 24,235-24,250, 1996.

Kim, J. H., and Newchurch, M. J., Climatology and trends of tropospheric ozone over the eastern Pacific ocean : the influences of biomass burning and tropospheric dynamics, *Geophys. Res. Lett.*, 23, 3723-3726, 1996.

Levine, J. S., T. D. Edwards, T. E. McReynolds, and C. W. Dull, Gaseous and particulate emissions from the fires in Kalimantan and Sumatra, Indonesia, *Report of WMO workshop on regional transboundary smoke and haze in South-East Asia*, World Meteorological Organization, Geneva, Switzerland, 1998.

Levine, J. S., The 1997 fires in Kalimantan and Sumatra, Indonesia : Gaseous and particulate emissions, *Geophys. Res. Lett.*, in press, 1999.

Liew, S. C., O. K. Kim, L. K. Kwok, and H. Lim, A study of the 1997 fires in South East Asia using SPOT quicklook mosaics, *Paper presented at the 1998 International Geoscience and remote sensing symposium*, Seattle, Washington, 3 pages, July 6-10, 1998.

Madronich, S., S. J. Flocke, J. Zeng, and I. Petropavloskyh, *Tropospheric Ultraviolet-Visible Model (TUV) Version 4*, NCAR Tech. Note, in preparation, 1999.

Seiler, W., and P. J. Crutzen, Estimates of gross and net fluxes of carbon between the biosphere and the atmosphere from biomass burning, *Clim. Change*, 2, 207-247, 1980.

Thompson, A. M., K. E. Pickering, D. P. McNamara, M. R. Schoeberl, R. D. Hudson, J. H. Kim, E. V. Browell, V. W. J. H. Kirchhoff, and D. Nganga, Where did tropospheric ozone over southern Africa and the tropical Atlantic come from in October 1992 ? Insights from TOMS, GTE TRACE A, and SAFARI 1992, *J. Geophys. Res.*, 101, 24,251-24,278, 1996.

Yokelson, R. J., R. Susott, D. E. Ward, J. Reardon, and D. W. T. Griffith, Emissions from smoldering combustion of biomass measured by open-path Fourier transform infrared spectroscopy, *J. Geophys. Res.*, 102, 18,865-18,877, 1997.

Table 1. Total and per-ecosystem emissions considered in MOZART to account for the 1997 Indonesian fires (based on Levine et al. [1999]). Global and annual biomass burning emissions in the model are also given for comparison.

Species	Forest	Agricultural	Peat	Indonesian Fires	Base case global
CO ₂ (TgC)	11.08	9.23	171.17	191.48	2963.2
CO (TgC)	0.94	0.78	31.07	32.79	283.6
CH ₄ (TgC)	0.17	0.04	1.78	1.99	29.5
NMHCs (TgC)	0.23	0.05	3.32	3.60	37.6
NO _x (TgN)	0.03	0.02	5.85	5.90	7.5

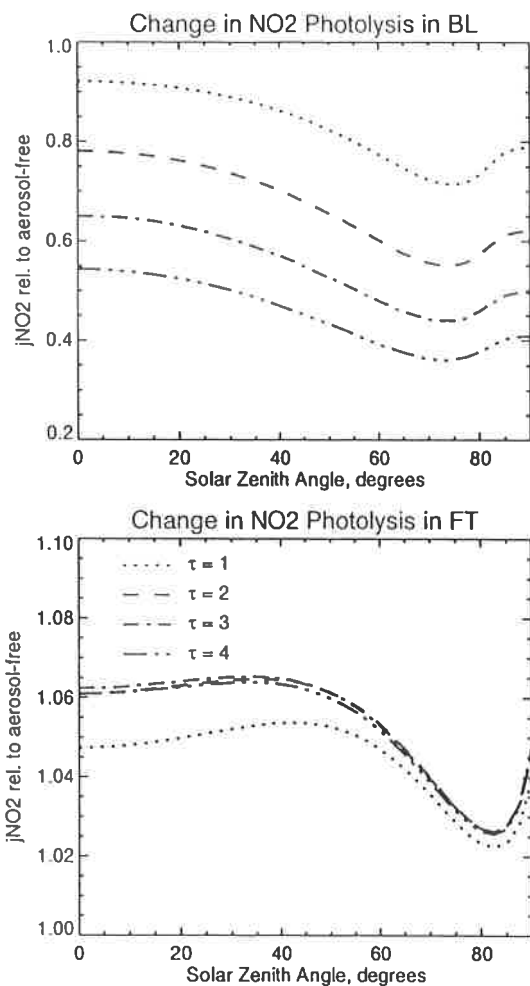
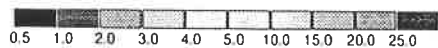
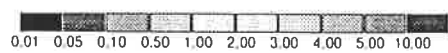
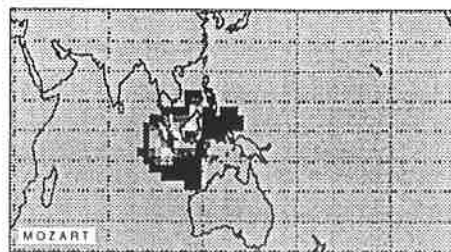


Figure 1: Calculated change in NO₂ photolysis rates for an uniform smoke aerosol ($\omega_0=0.88$) layer in the boundary layer (0-2km), relative to aerosol-free conditions. Different aerosol optical depths ($\tau = 1, 2, 3, 4$) are considered. The changes in j_{NO_2} are averaged over the boundary layer (BL) height (0-2km) or the free troposphere (FT).

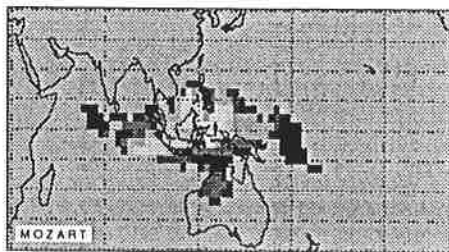
A/ O₃ Tropospheric Column Change (DU), 25 November



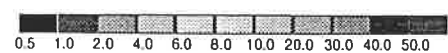
B/ NO₂ Column Change (10^{16} molec./cm²), 25 November



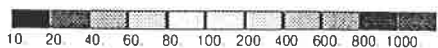
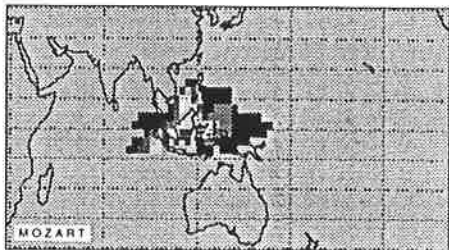
C/ Ozone Change (ppbv), Surface, 25 November



D/ Ozone Change (ppbv), 500 mb, 25 November



E/ CO Change (ppbv), Surface, 25 November



F/ CO Change (ppbv), 500 mb, 25 November

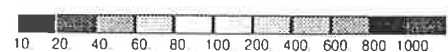


Figure 2: Calculated change in (A) tropospheric ozone column (DU: Dobson Units), (B) NO₂ total column (10^{16} molec./cm²), (C) ozone surface mixing ratio, (D) ozone 500 mb mixing ratio, (E) CO surface mixing ratio, and (F) CO 500 mb mixing ratio (ppbv) due to the Indonesian fire emissions. The change are presented for November 25 conditions. Note the different color scales.

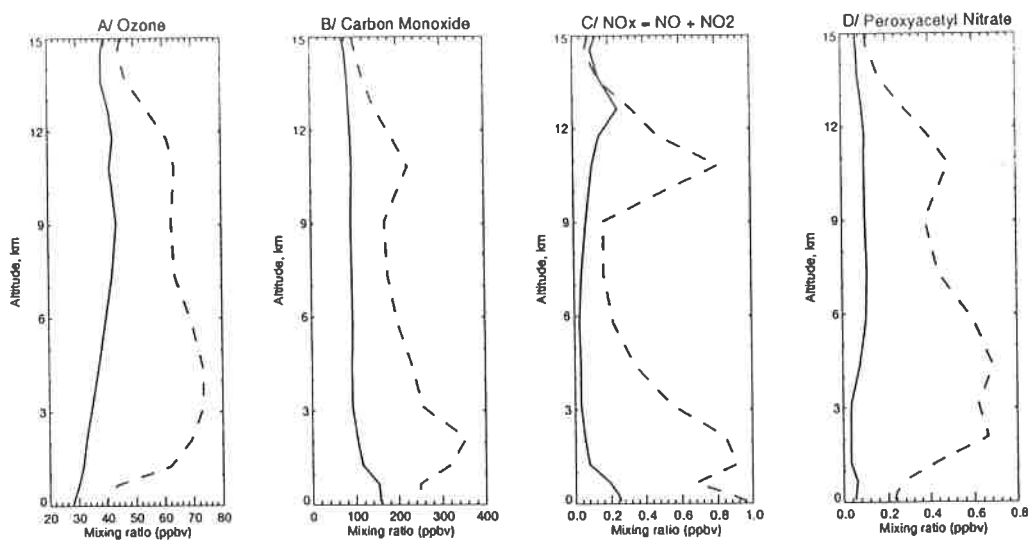


Figure 3: Vertical distributions of O₃, CO, NO_x, and PAN mixing ratio (ppbv) simulated for the base case (solid line) and for the 1997 fires case (dashed line) for November 25 conditions. The profiles are geographically averaged over the region 1.5°S-1.5°N in latitude and 107°E-110°E in longitude.

Partie 2

On the Essential Role of NO_x from Lightning in the Formation of Tropospheric Ozone Plumes in the Tropics

Didier Hauglustaine, Louisa Emmons, Mike Newchurch, Guy Brasseur, Toshinori Takao, Kouji Matsubara, James Johnson, Brian Ridley, Jeff Stith, and James Dye*

A series of ozone transects measured each year from 1987 to 1990 over the western Pacific and eastern Indian Oceans between mid-November and mid-December shows a prominent ozone maximum reaching 50-80 ppbv between 5 and 10 km in the 20°S-40°S latitude band. This maximum contrasts with ozone mixing ratios lower than 20 ppbv measured at the same altitudes in equatorial regions. Analyses with a global chemical transport model suggest that these elevated ozone values are part of a large-scale tropospheric ozone plume extending from Africa to the western Pacific across the Indian Ocean. These plumes occur several months after the peak in biomass burning influence and during a period of high lightning activity in the Southern Hemisphere tropical belt. The composition and geographical extent of these plumes are similar to the ozone layers previously encountered during the biomass burning season in this region. Our results indicate that production of nitrogen oxides from lightning strokes is essential in sustaining the NO_x ($=\text{NO}+\text{NO}_2$) levels and the ozone photochemical production required in the upper troposphere to form these persistent elevated ozone layers.

*D. Hauglustaine, Service d'Aéronomie du CNRS, Paris, France. L. Emmons, G. Brasseur, B. Ridley, Atmospheric Chemistry Division, NCAR, Boulder, CO. M. Newchurch, Department of Atmospheric Science, University of Alabama in Huntsville. T. Takao, K. Matsubara, Japan Meteorological Agency. J. Johnson, NOAA/PMEL, Seattle, WA. J. Stith, University of North Dakota, Grand Forks, ND. J. Dye, Mesoscale and Microscale Meteorology, NCAR, Boulder, CO.

Biomass burning and land-use practices in the tropics release large amounts of CO_2 and aerosols into the atmosphere and also constitute a major source of chemically active trace gases (e.g., CO , CH_4 , non methane hydrocarbons, NO_x) leading to the photochemical production of tropospheric ozone¹. Several model studies have indicated that trace gases emitted from tropical biomass burning can profoundly affect the budget and distribution of ozone and its precursors on the regional and even global scales². Satellite observations have identified elevated tropospheric ozone extending from Africa and South America into the South Atlantic and eastern Pacific Oceans during the biomass burning season³. Ground and airborne measurements during several field expeditions in the tropics have also demonstrated that biomass burning has a pervasive influence on the composition of the troposphere during the dry season⁴. The most prominent illustration of this influence is the formation of large-scale coherent plumes of tropospheric ozone and biomass burning products in the most pristine regions of the atmosphere during the peak in fire activity⁵. Since ozone is the precursor molecule for the hydroxyl radical (OH), which is the main oxidant in the atmosphere⁶, ozone increase resulting from biomass burning activities can affect the oxidizing efficiency of the atmosphere and the photochemical lifetime of species that are largely determined by oxidation in the tropical troposphere. Furthermore, the ozone greenhouse effect is most sensitive to ozone increments that occur in the tropical upper troposphere⁷, and hence tropical biomass burning is believed to provide a substantial radiative forcing of climate⁸.

A series of ozonesondes were launched from the research vessel *Shirase* by members of the Japanese Antarctic Research Expedition team during voyages from Japan to Antarctica across the western Pacific and eastern Indian Oceans between mid-

November and mid-December each year from 1987 to 1990⁹. The ozone profiles have been used to construct transect (latitude-altitude) distributions in this region of the troposphere for the four years of observation. Fig. 1a-d shows the resulting ozone mixing ratio together with the tropopause height, determined from the temperature profiles measured by the sondes¹⁰. The ozone volume mixing ratio in the marine boundary layer is generally below 20-30 ppbv. Very low mixing ratios (O_3 lower than 10 ppbv) were detected in 1988 in the marine boundary layer between 0°-20°N where ozone photochemical destruction prevails. Due to intense convective activity and vigorous updrafts in the rising branch of the Walker circulation, the middle and upper troposphere is characterized by low mixing ratios (10-20 ppbv) where the inter-tropical convergence zone (ITCZ) is located¹¹. In contrast, higher ozone mixing ratios (50-80 ppbv) occur in the middle and upper troposphere (5-10 km) in the region 20°S-40°S. This salient feature appears repeatedly from 1987 to 1990 during this period of the year. The tropopause is located at 16-17 km in the tropics, presents a discontinuity in the subtropics at 20°S-40°S, and decreases to 8-10 km south of 40°S. The high ozone values apparent in the profiles appear clearly in the tropospheric column amount depicted in Fig. 1f, showing values of 40-50 DU¹² at 20°S-40°S and a decrease to a minimum of 10-20 DU at the equator. Also shown are the tropospheric columns determined from the spaceborne TOMS (Total Ozone Mapping Spectrometer) instrument using the convective cloud differential technique for November 1987-1990¹³. The satellite observations range from 25 DU at 10°N to 30 DU at 10°S. Additional data from ozonesondes launched from the NOAA research vessel *Discoverer* during the ACE.1 (Aerosol Characterization Experiments) campaign as it cruised from Seattle to Tasmania

(mostly across the western Pacific Ocean south of 20°N) in November-December 1995¹⁴ is useful in identifying the extent of the ozone maximum observed during the *Shirase* cruise at 20°S-40°S. As depicted in Fig. 1e, the *Discoverer* ozonesonde data shows a similar feature east of the dateline with ozone mixing ratios reaching 50-100 ppbv at 20°S-40°S in the middle and upper troposphere and the tropospheric ozone column reaching 40 DU (Fig. 1f) in this region.

In order to provide more insight into the extent and origin of this persistent ozone maximum observed in the middle and upper troposphere at 20°S-40°S, results from the global chemical transport model MOZART¹⁵ (Model for Ozone and Related Chemical Tracers) have been sampled along the *Shirase* cruise track for the same period of the year (mid-November to mid-December). The ozone distribution calculated during this period, and illustrated in Fig. 2a, also shows a persistent maximum of 50-70 ppbv in the mid-upper troposphere around 30°S. The simulated tropospheric O₃ column is compared with the observations in Fig. 1f, and exhibits a mean value of about 30 DU (ranging from about 20 DU to 40 DU) at this latitude. The ozone cross-section from the model is also characterized by low values (lower than 20 ppbv) in the marine boundary layer south of 40°S and in the equatorial region, contrasting sharply with the maximum predicted and observed at 20°S-40°S. Intrusion from the stratosphere contributes only 30-40% of the ozone maximum and influences only the upper troposphere as indicated by the stratospheric component¹⁶ of ozone calculated by MOZART (Fig. 2b). Two additional model simulations help identify the origin of the ozone maximum. As shown in Fig. 2c, when the surface emissions of tropospheric ozone precursors (CH₄, CO, nonmethane hydrocarbons, NO_x) by savanna burning and by fires associated with

deforestation are omitted in the model¹⁷, the magnitude of the ozone maximum is reduced and mixing ratios of 40-50 ppbv are predicted between 5-10 km. This relatively uniform ozone decrease indicates that biomass burning emissions contribute 20-40% of the O₃ maximum predicted during this season. Although the peak in the burning season occurs approximately two months earlier, significant burning activity remains in November. The pattern of tropical fire activity as detected by satellite indicates that extensive burning takes place in July-September in the Southern Hemisphere tropical belt¹⁸. During the November-December period analyzed in this study, the most intensive burning appears in northern Africa savanna regions, although significant fire activity also occurs in southern Africa. In another sensitivity simulation (Fig. 2d), the model calculates ozone without including emission of nitrogen oxides from lightning activity. The NO_x lightning emission in the model¹⁹ totals 7 Tg-N/yr on a global and annual mean basis and is distributed according to the occurrence of deep convection as predicted by the NCAR Community Climate Model. Interestingly, in this case the calculated distribution of ozone along the *Shirase* cruise track (Fig. 2d) shows much lower ozone mixing ratios, with a uniform value of only 20-30 ppbv in the mid- and upper-troposphere at 20°S-40°S in November-December. Similar results (not shown) are obtained when the model results are sampled along the *Discoverer* cruise track in the western Pacific Ocean. Emissions of NO_x in the upper troposphere, and its subsequent meridional transport across the tropopause subtropical discontinuity, result in calculated stratospheric ozone tracer mixing ratios (Fig. 2b) higher by about 10-20 ppbv in the upper troposphere than ozone mixing ratios calculated for the *no-lightning* case (Fig. 2d).

Figure 3 presents a different perspective on the modeled distribution of species in the mid-troposphere and displays the O_3 mixing ratio over South America, Africa and the Indian Ocean at an altitude of 8 km. The ozone maximum encountered along the *Shirase* cruise track (depicted in Fig. 3 as white asterisks) over the eastern Indian Ocean at 20°S-40°S is part of a 1500-km wide ozone plume, characterized by O_3 mixing ratios reaching 60-80 ppbv, emanating from South Africa (and to a lesser extent from South America), and extending across the south Atlantic Ocean, the Indian Ocean and the western part of the Pacific Ocean. This plume contrasts with the low mixing ratios (less than 20 ppbv) calculated in the equatorial convective regions over the western Pacific and Indian Oceans. The associated NO_x emission (vertically integrated from the ground to the top of the convective clouds) from lightning in MOZART (Fig. 3b) indicates spots of high convective activity over South America, southern Africa, Madagascar, Indonesia, and Australia during this period. The model adequately captures the seasonally varying regional distribution of observed patterns of lightning. As revealed by global lightning flashes observed from spaceborne sensors²⁰, lightning primarily occurs in the inter-tropical convergence zone over continental regions in the summer hemisphere, and migrates north and south of the equator with the changing seasons, peaking over southern Africa, Madagascar, and Australia in December-February. The simulated NO_x ($=NO+NO_2$) distribution at 8 km clearly shows the influence of *in situ* lightning production on the nitrogen oxides mixing ratio with values reaching 200-300 pptv over the source region and 50-80 pptv downstream of the emission. Outside the plumes NO_x mixing ratios of 10-30 pptv are generally calculated over the ocean. Concomitant high peroxyacetyl nitrate (PAN) mixing ratios are calculated in the plumes (an excess of 100-150 pptv of PAN is calculated over the Indian Ocean plume in

comparison to the *no-lightning* simulation). PAN is photochemically produced from nonmethane hydrocarbons and NO_x released at the surface by combustion processes and/or the continental biosphere that are vented to the upper troposphere. Because the tropospheric ozone photochemical formation is generally NO_x -limited in the free troposphere, the distribution of the net ozone photochemical production²¹ follows the NO_x patterns (Fig. 3d). Over source regions (e.g., southern Africa) the net production reaches 5-10 ppbv per day, and lower values of 0.5-1.5 ppbv per day are calculated within the plumes. At this altitude where ozone loss processes are smaller, a net O_3 production of 0.1-0.5 ppbv per day is generally calculated in remote regions outside the plumes.

Over regions characterized by deep convective activity and lightning emissions (e.g., highlighted in Fig. 3b-c over South Africa), the collection of 24-h averaged NO_x profiles calculated by MOZART exhibits high mixing ratios in the boundary layer due to direct surface emissions, and reaches 500-1000 pptv (Fig. 4a). A secondary maximum is also predicted in the upper troposphere around 12 km near the top of the convective anvils. This secondary maximum is highly variable in space and time, and ranges from 100 pptv to about 800 pptv over this specific region (32°S-20°S; 20°E-30°E). For comparison, NO profiles measured within and about deep convective clouds during the TRACE-A campaign²² in September-October 1992 over South America, the south Atlantic and southern Africa (Fig. 4b), during the ELCHEM campaign²³ in July-August 1989 over New Mexico (Fig. 4c) and within thunderstorms during STERAO/Deep Convection²⁴ in June-July 1996 over Colorado (Fig. 4d) are also displayed.²⁵ The ELCHEM and STERAO observations were collected at latitudes of 30°N-40°N characterized by low tropopause height and low convective cloud tops in comparison to

the tropical profiles calculated over South Africa by the MOZART model. Despite this difference, the observations clearly show a variable maximum in the upper troposphere with NO_x mixing ratios reaching 800-1000 pptv during ELCHEM and as high as 3000 pptv during STERAO directly inside the anvil region of electrically active convective towers (which includes some contribution from boundary layer sources of northeastern Colorado). A similar highly variable maximum in NO mixing ratio reaching 800 pptv at 10-12 km was also observed during TRACE-A over biomass burning and convective regions (Fig. 4b). In contrast, over the region of interest in southern Africa, the profiles calculated by MOZART for the *no-lightning* case (not shown) are characterized by a typical *C-shape* with mixing ratios of 800-1000 pptv in the boundary layer decreasing to less than 50 pptv at 5 km, constant throughout the free troposphere, and increasing with height above 13-15 km due to stratospheric influence. In the absence of lightning, the calculated NO_x concentrations are below 20-30 pptv in the upper troposphere, and ozone decreases below 30-40 ppbv at 8-10 km. As illustrated in Fig. 2, the large-scale redistribution of lightning NO_x can also affect ozone in the lower stratosphere.

In this study, large-scale ozone plumes observed in the remote middle and upper troposphere over the eastern Indian Ocean and western Pacific have been presented. These ozone plumes were observed several months after the peak of biomass burning influence and during high convective and lightning activity in the Southern Hemisphere tropical belt. In accordance with previous modeling work²⁶, results from a chemical transport model of the atmosphere indicate that lightning is the primary source of NO_x in the mid- and upper-troposphere over a large portion of the Southern Hemisphere during this period. Our results further suggest that during the season of interest (i.e., Southern Hemisphere summer), injection of nitrogen oxides by lightning activity over the

continents sustains the NO_x levels in the middle and upper tropical troposphere, leading to substantial photochemical production of ozone (and PAN). The air is then transported aloft in the subtropical jet stream, resulting in large-scale ozone plumes over remote oceanic regions as observed during the *Shirase* and *Discoverer* cruises. We propose that the same dominant role of lightning injection in sustaining the NO_x levels in the upper troposphere can be extended to the September/October period. This conclusion would imply the essential role of lightning NO_x in the formation of large-scale tropospheric ozone plumes in the Southern Hemisphere tropical belt, persisting from September/October until November/December.

References and Notes

- ¹ Chameides, W., and J. C. G. Walker, *J. Geophys. Res.*, 78, 1973; Seiler, W., and P. J. Crutzen, *Clim. Change*, 2, 207 (1980); Crutzen P. J., L. E. Heidt, J. P. Krasnec, W. H. Pollock, and W. Seiler, *Nature*, 282, 253 (1979); Crutzen, P. J., W. M. Hao, M. H. Liu, J. M. Lobert, and D. Scharffe, in «*Our Changing Atmosphere*», pp. 449-471 (1989).
- ² Bonsang, B., M. Kanakidou, and C. Boissard, in «*Non-CO₂ greenhouse gases*», pp. 261-270 (1994); Granier, C., W. M. Hao, G. Brasseur, and J. F. Muller, in «*Biomass Burning and Global Change*», pp. 140-148 (1997); Chatfield, R. B., J. A. Vastano, H. B. Singh, and G. Sachse, *J. Geophys. Res.*, 101, 24279 (1996); Roelofs, G.-J., J. Lelieveld, H. G. J. Smit, and D. Kley, *J. Geophys. Res.*, 102, 10637 (1997); Hauglustaine, D. A., G. P. Brasseur, and J. S. Levine, in «*Biomass Burning and its Interactions with the Climate System*», in press (1999).
- ³ Fishman, J. K., Fakhruzzaman, B. Cross, D. Nganga, *Science*, 252, 1693 (1991); Kim, J. H., and M. J. Newchurch, *Geophys. Res. Lett.*, 23, 3723 (1996); Ziemke, J. R., S. Chandra, and P. K. Bhartia, *J. Geophys. Res.*, 103, 22115 (1998); Hudson, R. D., and A. M. Thompson, *J. Geophys. Res.*, 103, 22129 (1998).
Kim, J.H., and M.J. Newchurch, *J. Geophys. Res.*, 101, 1455, 1998.
- ⁴ Logan, J. A., and V. W. J. H. Kirchhoff, *J. Geophys. Res.*, 91, 7875 (1986); Smit, H. G. J., S. Gilde, and D. Kley, in «*Physico-Chemical Behaviour of Atmospheric Pollutants*», pp. 630-637 (1990); Kley, D., *Science*, 276, 1043 (1997); Cros, B., D., Nganga, A. Minga, J. Fishman, and V. Brackett, *J. Geophys. Res.*, 95, 12869 (1992); Baldy, S., G. Ancellet, M. Besafi, A. Badr, and D. Lan Sun Luk, *J. Geophys. Res.*, 101, 23835 (1996); Thompson, A. M., et al., *J. Geophys. Res.*, 101, 24251 (1996); Jonquière, I., A. Marengo, A. Maalej, F. Rohrer, *J. Geophys. Res.*, 103, 19059, 1998, Schultz, M., et al., *J. Geophys. Res.*, in press (1999).
- ⁵ Blake, D. R., et al., *Science*, in press (1999); D. Davis et al., *J. Geophys. Res.*, 101, 2111, 1996; I. Folkins, R. Chatfield, D. Baumgardner, M. Profitt, *J. Geophys. Res.*, 102, 13291, 1997.
- ⁶ Levy, II, H., *Science*, 173, 141 (1971).
- ⁷ Lacis, A. A., D. J. Wuebbles, and J. A. Logan, *J. Geophys. Res.*, 95, 9971 (1990); Hauglustaine, D. A., and C. Granier, in «*Atmospheric Ozone as a Climate Gas*», pp. 189-203 (1995); Forster, P. M. de F., and K. P., Shine, *J. Geophys. Res.*, 102, 10841 (1997).
- ⁸ Portmann, R. W., S. Solomon, J. Fishman, J. R. Olson, J. T. Kiehl, and B. Briegleb, *J. Geophys. Res.*, 102, 9409 (1997).
- ⁹ Matsubara, K., M. Doi, T. Uekubo, K. Okada, S. Aoki, and S. Kawaguchi, in *Proc. NIPR Symposium Polar Meteorol. Glaciol.*, 4, pp. 1-11, 1991; Japan Meteorological Agency, *Antarctic Meteorological Data obtained by the Japanese Antarctic Research Expedition*, Special Volume VI, Summary of Meteorological Observations at Syowa, Mizuho, and Asuka Stations 1961-1993, Tokyo (1995). The sondes used an electrochemical concentration cell (ECC, type RSII-KC79) for measuring ozone. Ozonesonde data is typically scaled to match concurrent total column measurements (ground based or satellite), and ECC sonde data requiring a scale factor outside the range 0.8-1.2 are discarded according to Logan, J. A. [*J. Geophys. Res.*, 99, 25553 (1994)]. Two of these 66 sondes in this data set have been left out of this analysis for that reason.
- ¹⁰ We adopt the World Meteorological Organization (WMO) thermal tropopause definition (i.e., the lowest altitude at which the temperature lapse rate decreases to 2K/km or less and remains below this value for a depth of at least 2 km).

¹¹ Kley, D., et al., *Science*, 274, 230 (1996); Kley D., et al., *Q. J. R. Meteorol. Soc.*, 123, 2009 (1997).

¹² 1 Dobson Unit (DU) = 2.69×10^{-6} molec. cm⁻².

¹³ Ziemke, J. R., S. Chandra, and P. K. Bhartia, *J. Geophys. Res.*, 103, 22115 (1998).

¹⁴ Bates, T. S., et al., *J. Geophys. Res.*, 103, 16297 (1998). The ACE 1 ozone soundings were made with an ECC-type EN-SCI sonde. The *Discoverer* data are reported every 0.25 km, in contrast to the 1-1.5 km resolution reported for the *Shirase* data.

¹⁵ MOZART (Model for ozone and related chemical tracers) is a three-dimensional chemical transport model (CTM) of the global troposphere described and evaluated by Brasseur G. P. et al. [*J. Geophys. Res.*, 103, 28265 (1998)] and Hauglustaine D. A. et al. [*J. Geophys. Res.*, 103, 28291 (1998)]. This model has been developed in the framework of the National Center for Atmospheric Research (NCAR) Community Climate Model (CCM). In MOZART (version 1), the time history of 56 chemical species is calculated on the global scale from the surface to the mid-stratosphere. The model accounts for surface emissions of chemical compounds (N₂O, CH₄, non methane hydrocarbons, CO, NO_x, CH₂O, and acetone), advective transport (using the semi-Lagrangian transport scheme of Williamson, D. L., and P. J. Rasch [*Mon. Weather Rev.*, 117, 102 (1989)]), convective transport (using the formulation of Hack, J. J. [*J. Geophys. Res.*, 99, 5551 (1994)]), diffusive exchanges in the boundary layer (based on the parameterization of Holtslag, A., and B. Boville [*J. Climate*, 6, 1825 (1993)]), chemical and photochemical reactions, wet deposition of 11 soluble species, and surface dry deposition. The chemical scheme includes 140 chemical and photochemical reactions and considers the photochemical oxidation schemes of methane (CH₄), ethane (C₂H₆), propane (C₃H₈), ethylene (C₂H₄), propylene (C₃H₆), isoprene (C₅H₈), terpenes (as α -pinene, C₁₀H₁₆), and a lumped compound n-butane (C₄H₁₀) used as a surrogate for heavier hydrocarbons. The evolution of species is calculated with a numerical time step of 20 min for both chemistry and transport processes. The model is run with a horizontal resolution which is identical to that of CCM (triangular truncation at 42 waves, T42) corresponding to about 2.8 degrees in both latitude and longitude. In the vertical, the model uses hybrid sigma-pressure coordinates with 25 levels extending from the surface to the level of 3 mb. Dynamical and other physical variables needed to calculate the resolved advective transport as well as smaller-scale exchanges and wet scavenging are pre-calculated by the NCAR CCM (version 2, $\Omega 0.5$ library), and provided every 3 hours from pre-established history tapes. A preliminary version of the model was used by Brasseur, G. P. et al. [*J. Geophys. Res.*, 101, 14795 (1996)] to investigate the budget of chemical compounds in the Pacific troposphere in conjunction with the MLOPEX measurements. More recent versions of the model were used by Hauglustaine, D. A., et al. [in «*Atmospheric Ozone*», pp. 735-738 (1998)] in a study of ozone over the North Atlantic ocean, and in Emmons, L. K., et al. [*Atmos. Environ.*, 31, 1851 (1997)] for a comparison of nitrogen species distributions provided by various CTMs and observed climatologies.

¹⁶ The stratospheric tracer in MOZART is imposed identical to the modeled «real» ozone above the model tropopause. Below the tropopause, no photochemical production is specified, and the photochemical loss is attributed to ozone photolysis followed by the reaction of O(¹D) with water vapor, to reaction of ozone with OH and HO₂, and to reaction of ozone with NMHCs. Dry deposition at the surface is also considered for the stratospheric tracer. A similar stratospheric ozone tracer definition has been used previously by Roelofs, G. -J., and J. Lelieveld [*Tellus*, 49B, 38 (1997)].

¹⁷ Biomass burning emissions in MOZART account for fires in tropical and non tropical forests, savanna burning, fuel wood use, and agricultural waste burning. The spatial and temporal distributions of the amount of biomass burned is taken from Hao, H. M., and Liu M.-H. [*Global Biogeochem. Cycles*, 8, 495 (1994)] in the tropics and from Müller, J.-F. [*J. Geophys. Res.*, 97, 3787 (1992)] in non tropical regions. The emission ratios of each species relative to CO₂ are taken from Granier, C., et al. [in «*Biomass Burning and Global Change*», pp. 140-148 (1997)] for each type of biomass fire except for the CO and NO_x (=NO+NO₂) from savanna where the values suggested by respectively Hao, W. M., et al. [*J. Geophys. Res.*, 101, 23577 (1996)] and by Andreae, M. O., et al. [in «*Biomass Burning and Global Change*», pp. 278-295 (1997)] are considered. The biomass burning emissions in the model total 283.6 Tg-C of CO,

29.5 Tg-C of CH₄, 37.6 Tg-C of NMHCs, and 7.5 Tg-N of NO_x on a global and annual mean basis. In the *no-biomass burning* simulation, these emissions are set to zero.

¹⁸ Cahoon, D. R., et al., *Nature*, 359, 812 (1992); Dwyer, E., J.-M. Grégoire, and J.-P. Malingreau, *Ambio*, 27, 175 (1998); See also the ESA Global Fire Atlas web site (<http://shark1.esrin.esa.it/FIRE/fire.html>).

¹⁹ There is clearly a need for more accurate lightning NO_x emission parameterizations in global chemical transport models [J. Penner et al., *J. Geophys. Res.*, 103, 22097, 1998]. The uncertainty on the global production of NO_x from lightning is considerable. Based on field campaigns, Huntrieser, H. [*J. Geophys. Res.*, 103, 28247, 1998], recently derived a range of 0.3-22 Tg-N/yr. The most recent theoretical and laboratory estimates of the global production are also quite variable and generally extrapolated to the global scale from a relatively limited number of local measurements (1-8 TgN/yr [Lawrence, M. G., et al., in *Atmospheric Electrodynamics*, pp. 189-202 (1995)], 3-5 Tg-N/yr [Levy, II, H., W. J. Moxim, and P. S. Kasibhatla, *J. Geophys. Res.*, 101, 22911 (1996)], 12.2 (5-20) Tg-N/yr [Price, C., J. Penner, and M. Prather, *J. Geophys. Res.*, 102, 5929 (1997)], 13.2 Tg-N/yr [Price, C., J. Penner, and M. Prather, *J. Geophys. Res.*, 102, 5943 (1997)], 5 TgN/yr [Lee, D. S. et al., *Atmos. Environ.*, 31, 1735 (1997)], 2.5 and 8.3 Tg-N/yr [Wang, Y., A. W. DeSilva, G. C. Goldenbaum, R. R. Dickerson, *J. Geophys. Res.*, 103, 19149 (1998)]). In MOZART, we use a global and annual NO_x production of 7 Tg-N/yr, distributed (possibly incorrectly) as a function of space and time according to the occurrence of deep moist convection in the NCAR CCM sampled every 3 hours, and following the empirical parameterization of Price, C., and D. Rind [*J. Geophys. Res.*, 97, 9919 (1992)] and cloud top heights statistics from the CCM. A further difficulty in the simulation of lightning emissions in the models arises from the vertical allocation of the NO_x injection. Our current understanding of NO_x formation in cloud-to-cloud and cloud-to-ground discharges is not sufficient to determine the relative contributions of these two processes. In MOZART, the lightning nitrogen production is distributed as a constant mass throughout the total column (from the ground to the cloud top). This assumption underestimates the potential role of cloud-to-cloud relative to cloud-to-ground discharges as NO_x producers. However, as illustrated by Gallardo, L., and V. Cooray [*Tellus*, 48B, 641 (1996)], Levy, II, H., W. J. Moxim, and P. S. Kasibhatla [*J. Geophys. Res.*, 101, 22911 (1996)], and Pickering, K., Y. Wang, W.-K. Tao, C. Price, and J.-F. Muller [*J. geophys. Res.*, 103, 31203 (1998)] assuming a higher efficiency of cloud-to-cloud discharges will result in a larger input of nitrogen in the upper part of the troposphere and an increased impact on ozone in this region.

²⁰ Turman, B. N., and B. C. Edgar, *J. Geophys. Res.*, 87, 1191 (1982); Orville, R. E., and R. W. Henderson, *Mon. Weather. Rev.*, 114, 2640 (1986); Christian, H. J., et al., in *Proceedings of the 10th International Conference on Atmospheric Electricity*, pp. 368-371 (1996); see also the Optical Transient Detector web site (<http://thunder.msfc.nasa.gov>).

²¹ The photochemical production of O₃ is mainly due to reaction of hydroperoxy or organic peroxy radicals with NO to form NO₂ which is further photolyzed during daytime to form O(³P) and subsequently ozone. Photochemical loss is principally attributed to ozone photolysis followed by the reaction of O(¹D) with water vapor, to reaction of ozone with OH and HO₂, and to reaction of ozone with NMHCs.

²² Smyth S. B. et al., *J. Geophys. Res.*, 101, 24165 (1996); D. Jacob et al., *J. Geophys. Res.*, 101, 24235, 1996.

²³ Ridley, B. A., J. G. Walega, J. E. Dye, and F. E. Grahek, *J. Geophys. Res.*, 99, 25519 (1994).

²⁴ STERAO (Stratospheric-Tropospheric Experiment: Radiation, Aerosols and Ozone)/Deep Convection was a multidisciplinary study of the production of NO_x by lightning and the transport and redistribution of chemical species in the troposphere by thunderstorms. Aircraft measurements were made in the upper troposphere in thunderstorm anvils and in the boundary layer. Doppler radar, a lightning interferometer and field change meters were employed to probe the microphysical and electrical properties of the storms. [Dye, J.E. et al., «An overview of the STERAO/Deep Convection Experiment with example results for the July 10th storm», *J. Geophys. Res.*, to be submitted]

²⁵ Plumes of NO from thunderstorms have also been observed over the north Atlantic [Brunner, D., J.

Stachelin, D. Jeker, *Science*, 282, 1305, 1998.

²⁶ Lamarque, J.-F., G. P. Brasseur, P. G. Hess, and J.-F. Muller, *J. Geophys. Res.*, 101, 22955 (1996); Levy II, H., W. J. Moxim, and P. S. Kasibhatla, *J. Geophys. Res.*, 101, 22911 (1996); Penner, J. E., et al., *J. Geophys. Res.*, 103, 22097 (1998).

²⁷ The National Center for Atmospheric Research is operated by the University Corporation for Atmospheric Research under the sponsorship of the National Science foundation. Support for J. Stith was provided by the National Science Foundation through grant ATM-9634125.

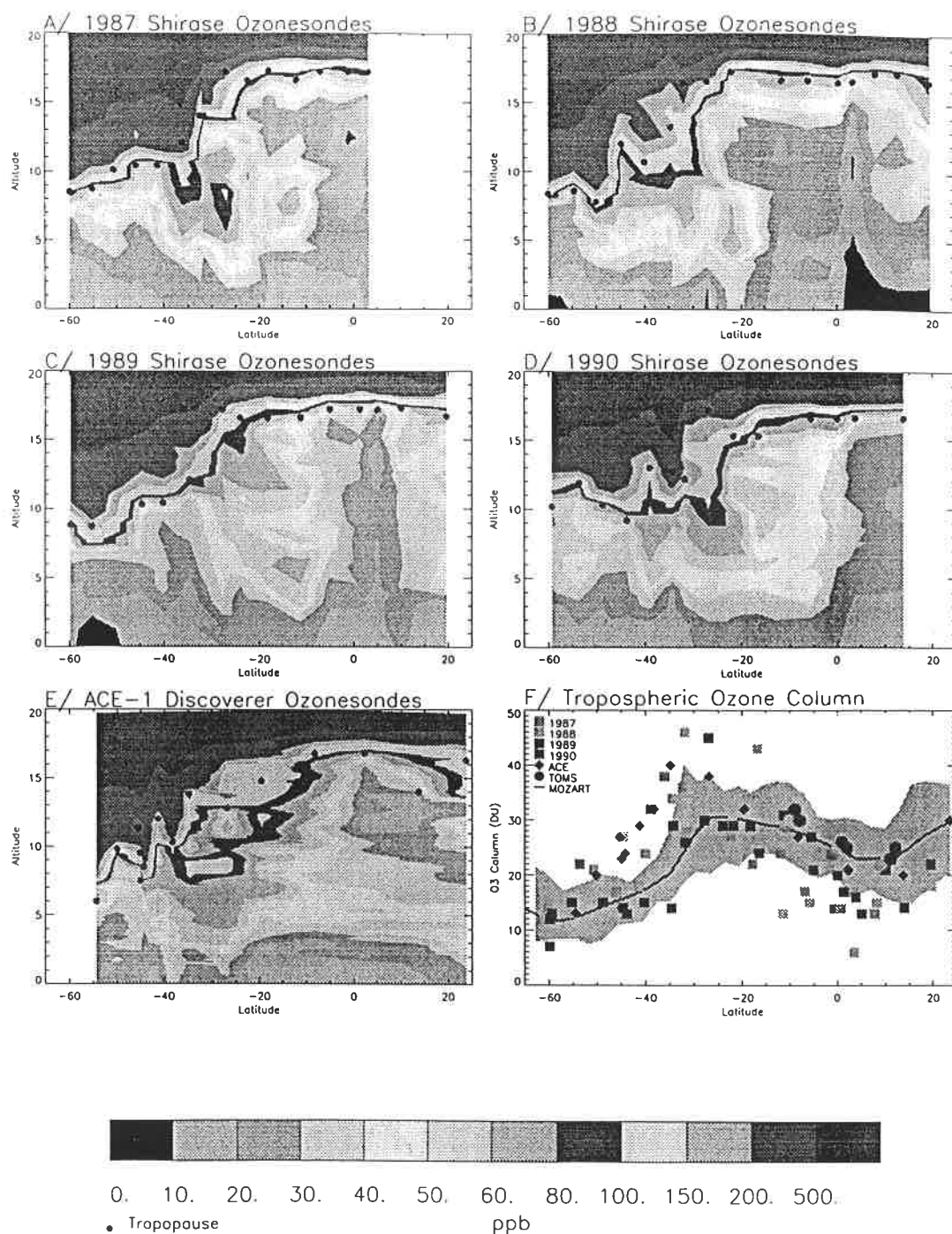


Figure 1: Ozone mixing ratio (ppbv) measured from ozonesondes during ship cruises plotted as a function of latitude and altitude, (A-D) From the research vessel *Shirase* 1987-1990 between Japan and Antarctica. (E) From the research vessel *Discoverer* during ACE-1 between California and Tasmania in 1995. (F) Tropospheric ozone columns calculated for the *Shirase* soundings (squares), and the ACE soundings (diamonds) along with tropospheric columns determined from TOMS for 1987-1990 (dots), and the results from MOZART for the *Shirase* cruise track location from mid-November to mid-December, shown by the solid line (mean) and shading (standard deviation).

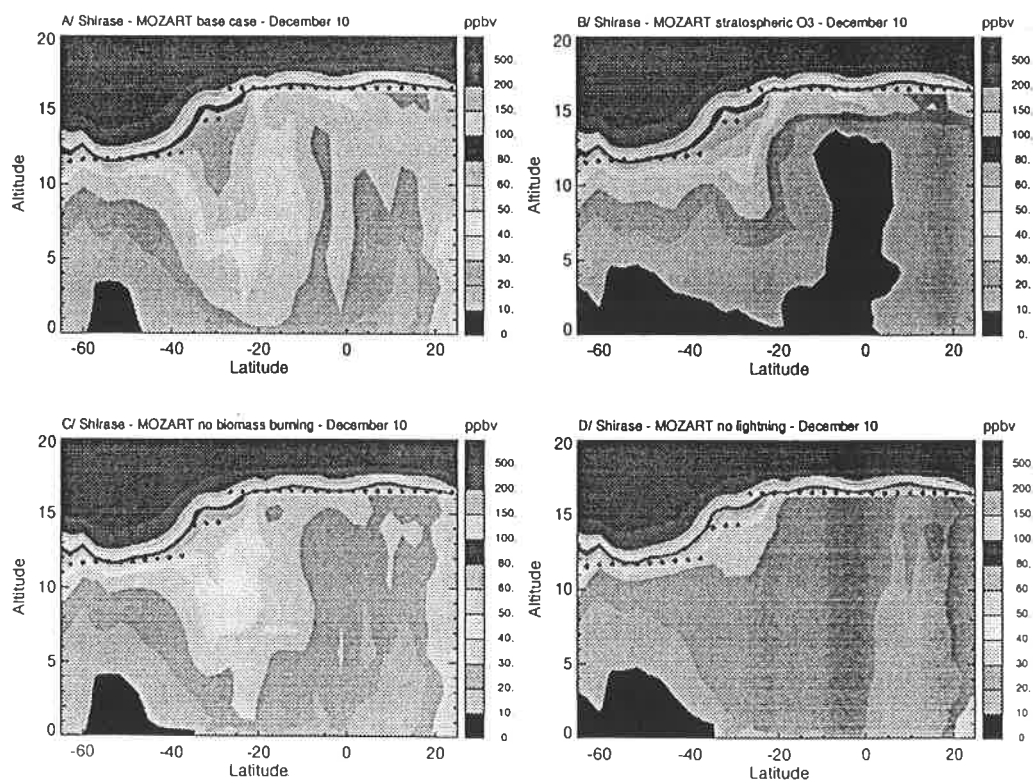


Figure 2: Ozone cross sections (ppbv) calculated by the MOZART global model sampled along the *Shirase* cruise track for December 10 conditions. (A) Ozone for the base case simulation. (B) Stratospheric ozone tracer for the base case simulation. (C) Ozone calculated without biomass burning emissions. (D) Ozone calculated without lightning NO_x emissions.

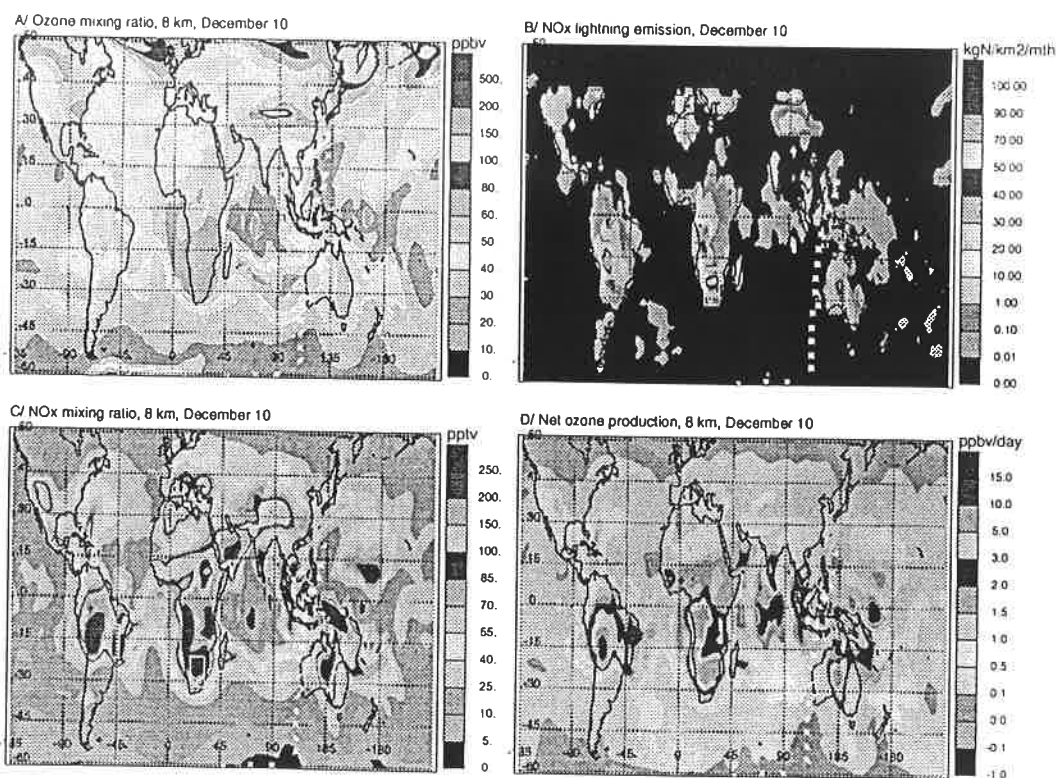


Figure 3: (A) Ozone from MOZART at 8 km altitude for December 10 conditions (ppbv). The asterisks indicate the location of the *Shirase* ozone soundings. (B) Lightning NO_x emissions from MOZART vertically integrated from the surface to the cloud top (kgN/km²/month). (C) NO_x mixing ratio from MOZART at 8 km altitude (pptv). (D) Net ozone photochemical production (24h average) calculated by MOZART at 8 km for December 10 (ppbv/day).

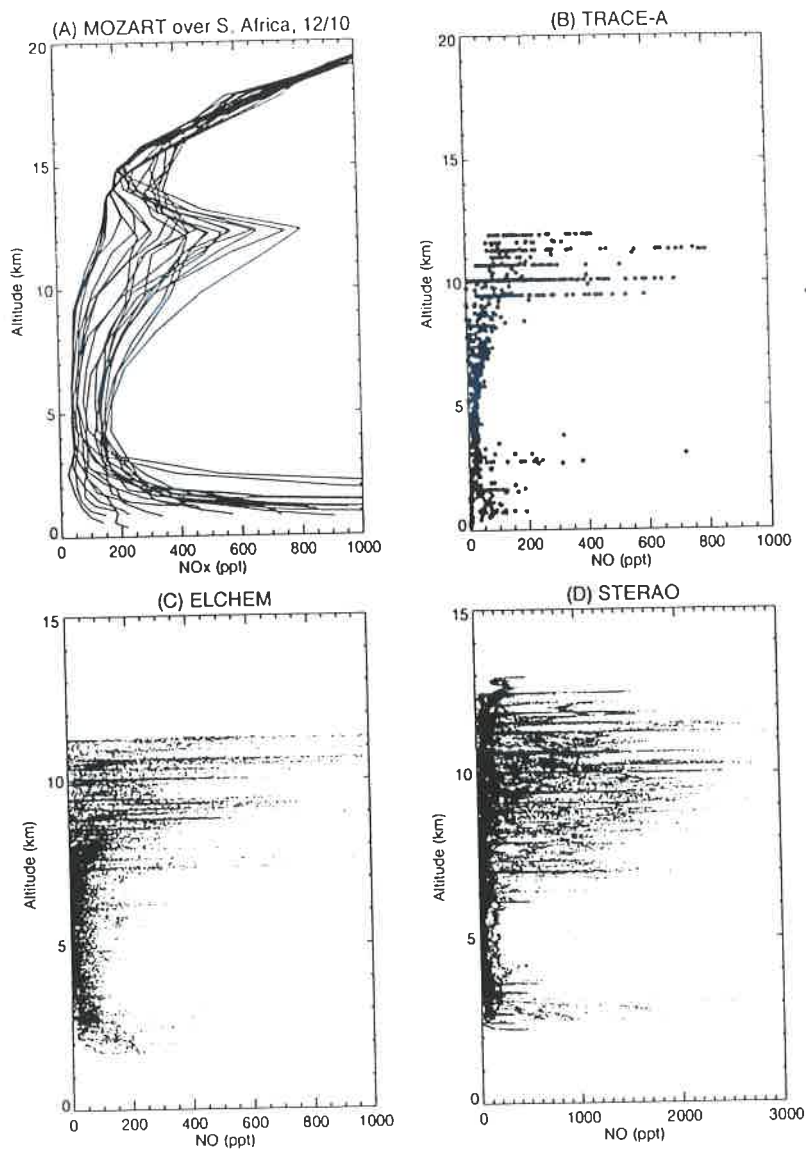


Figure 4: (A) NO_x vertical profiles from MOZART for the source region over southern Africa for December 10 conditions (pptv). The location of the model profile sampling is indicated by the white box in Fig. 3. (B) NO profiles observed during TRACE-A over South America, South Atlantic and southern Africa. (C) Vertical distribution of NO observed during ELCHEM within and about convective clouds over New Mexico. (D) STERAO NO profiles observed in thunderstorms in Colorado.